

# Direction finding accuracy of sequential lobing under target amplitude fluctuations

Çağatay Candan, Sencer Koç

Department of Electrical-Electronics Engineering, METU, 06531 Ankara, Turkey  
E-mail: ccandan@metu.edu.tr

**Abstract:** Using recently developed statistical target fluctuation models, the accuracy of sequential lobing is analytically studied. The study shows that the sequential lobing method suffers from a significant performance loss, in comparison with the monopulse method, for the Rayleigh fluctuation model. For other fluctuation models, the performance loss gradually decreases as the amplitude spread associated with the fluctuation gets smaller. The present study aims to analytically quantify the mentioned accuracy loss because of target amplitude fluctuation and aims to assess the engineering utility of the sequential lobing method for practical applications. To that aim, two operational regimes, namely the noise-limited and target-fluctuation-limited operational regimes, are introduced and the boundary between regimes, separating acceptable and unacceptable performance loss with respect to monopulse method, is analytically determined.

## 1 Introduction

Sequential lobing is a well-established direction finding technique based on successively switching the transmitter beam between two positions to obtain the target angular position. This technique, with its modest calibration and hardware requirements, is commonly adopted in early radar systems and is still being preferred in some modern systems because of its implementation advantages [1, p. 224]. The goal of this paper is to quantify the direction finding accuracy of the sequential lobing technique.

As noted by Skolnik [1, Fig. 4.16], the performance of sequential lobing is expected to deteriorate for manoeuvring targets. To the best of our knowledge, the amount of deterioration, its variation with signal-to-noise ratio (SNR; or equivalently target range) and a performance comparison with other techniques, that is, monopulse methods, are not quantitatively given in the literature. In this study, our goal is to use recently suggested statistical target fluctuation models to present a justification of the qualitative comments given by Skolnik [1, Fig. 4.16].

Direction finding is one of the fundamental tasks of radar systems. Early systems equipped with a single beam are required to switch the beam in two different positions, that is, illuminate the target once, switch the beam to a squinted position and then illuminate the target once more, so as to obtain information about the target angular position. The described operation is illustrated in Fig. 1. The fundamental assumption of the sequential lobing is the constancy of target amplitude for the total duration comprising both illuminations. The illumination times are indicated as  $T_1$  and  $T_2$  in Fig. 1. With this assumption, the target angular position is estimated using the knowledge of antenna patterns.

In contrast to sequential lobing, monopulse systems simultaneously process the return with multiple receivers and the target angular position is extracted from a single radar pulse (possibly burst of pulses). The name 'monopulse' follows from the described mode of operation. Owing to the instantaneous data gathering, the monopulse systems are not affected by the target fluctuation. This is the main advantage of monopulse systems. Unfortunately, the hardware complexity and calibration requirements of the monopulse systems are more demanding than sequential lobing systems and this is the main reason that the sequential lobing technique is still being utilised in spite of its questionable performance for manoeuvring, that is, fluctuating targets. One of the goals of this study is to analytically evaluate the practical 'value' of sequential lobing for manoeuvring targets.

The literature on the performance of sequential lobing technique is quite limited. The most important study in this line is the work of Lo [2], which presents an examination of a practical implementation. This study focuses on a system with a logarithmic amplifier in the radio frequency (RF) chain and assumes that the output of the logarithmic amplifier for two beams is statistically independent. The independence assumption is based on the assumed target model (non-fluctuating target) and independence of receiver noise in two receptions.

A recent work of Cui *et al.* [3] extends the work of Lo to the fluctuating targets and examines the sequential lobing performance for a non-coherent receiver with a logarithmic amplifier. In the present study, we examine the same problem for a coherent receiver and place a particular emphasis on the quantification of the performance loss between monopulse and sequential lobing methods. More specifically, the main goal of this study is to assess the

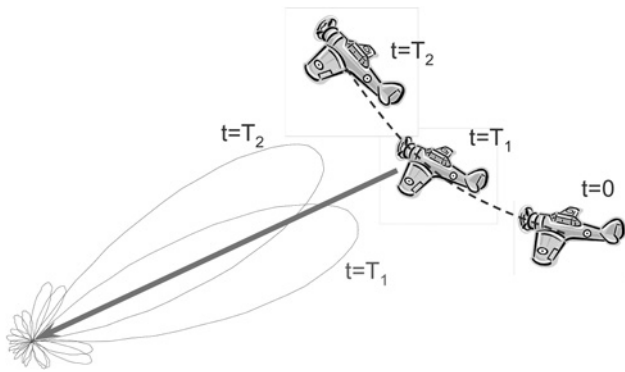


**Fig. 1** Illustration for the operation of sequential lobing technique with manoeuvring targets

practical value/utility of sequential lobing, in comparison with the monopulse, for modern systems. To this aim, we introduce two operational regimes namely the target-fluctuation-limited and the noise-limited regimes and establish the connection between the target fluctuation models and the operational regimes. In contrast to the sequential lobing literature, the monopulse literature is significantly richer. One can consult [4–6] for various aspects of monopulse systems. To the best of our knowledge, the examined problem has not been studied in the open literature apart from recent work of Cui *et al.* [3] complementing the findings herein.

## 2 Statistical target fluctuation models

We use the generalised gamma distribution as the target fluctuation model. The model encompasses some other well-known fluctuation models such as Swerling, Weibull models and can be considered as the generalised Swerling model [7]. A number of target models and their connections

are presented in Fig. 2. Here, we use the bivariate generalised gamma distribution to model the target amplitude at time instants  $T_1$  and  $T_2$  of sequential lobing.

The bivariate generalised gamma distribution has the shape parameters (also known as Nakagami fading parameter)  $m_1, m_2$ ; the scale parameters  $\Omega_1, \Omega_2$ ; the correlation parameter  $\rho$  and the exponent parameters  $\nu_1, \nu_2$  as shown in Fig. 2. The generality of the distribution results in fairly complicated analytical expressions for its probability density function and cumulative density function. The expressions for these functions can be found in [8, eq. (2) and eq. (4)]. In this work, we refrain from presenting these relations, but instead emphasise the connections with more familiar distributions to convey the process of target amplitude modelling.

We start with a brief review of some facts about the gamma distribution. A gamma distributed random variable can be considered as the summation of independent and identically distributed (i.i.d.) zero-mean Gaussian random variables, that is  $\sum_{k=1}^{2m} (x_k)^2$ , where each  $x_k$  is i.i.d. Gaussian distributed with zero mean and variance  $\sigma_x^2$  [9, eq. (29)]. When the shaping parameter  $m$  is an integer multiple of  $1/2$ , the gamma distribution is identical to the  $\chi^2$  distribution with  $2m$  degrees of freedom. The parameter  $m$  ( $m \geq 1/2$ ) relates to the fading of the signal and called as the fading parameter or Nakagami- $m$  parameter in the communication studies [10]. As  $m \rightarrow \infty$ , the effect of fading is monotonically reduced, that is, the variance of the distribution reduces and the distribution gets concentrated around the mean.

The generalised gamma distribution is related to the standard gamma distribution through a simple ‘power relation’. If  $y$  is gamma distributed, then the variable  $r = y^{1/(2\nu_i)}$  for  $\nu_i > 0$  is said to be generalised gamma distributed. It should be noted that when parameter  $\nu_i$  is taken as  $1/2$ , the generalised gamma distribution reduces to the standard gamma distribution. The power relation is especially important for the Weibull model where the exponent  $\nu_i$  is adjusted to match the spikiness of the

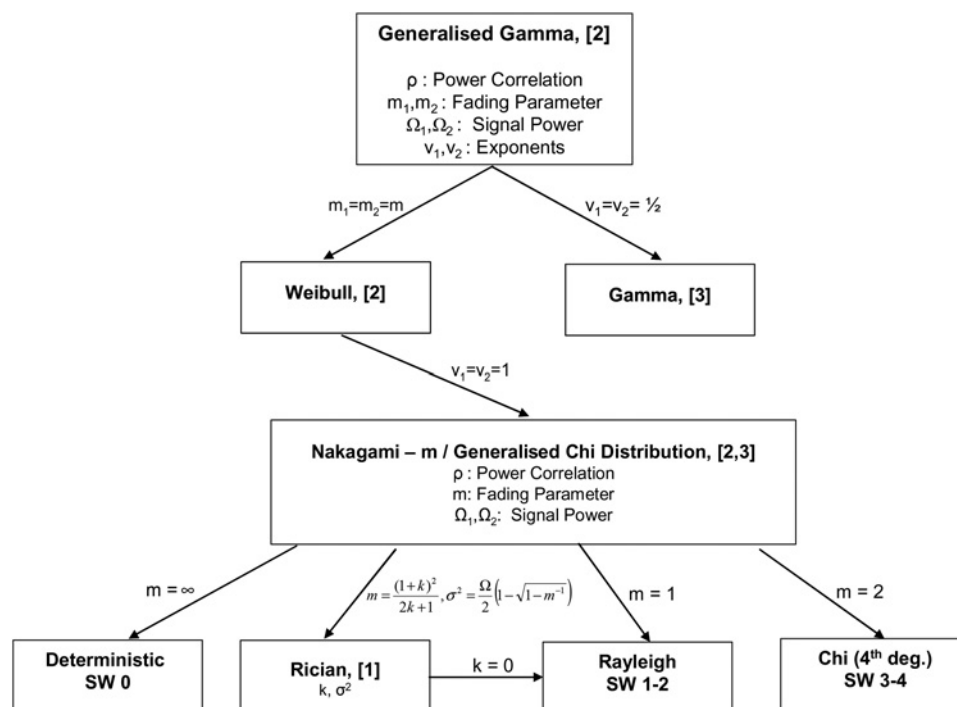


**Fig. 2** Statistical models for target amplitude fluctuation and their connection with generalised gamma model

collected data. In this study, we are interested in the comparison of the amplitude or equivalently the power (amplitude square) of two signals received in succession; therefore the choice for the exponent  $v_i$  is not critical for the present study.

We would like to remark that in radar signal processing, the  $m$ -parameter is related to the spread of the amplitude fluctuation and the parameter  $\Omega_k$  represents the mean value of the return power. Hence, the gamma variate characterises the power return of the target. It should also be remarked that the square root of gamma variate corresponds to the Nakagami- $m$  distribution and said to represent the ‘voltage signal’ according to the electrical engineering terminology.

The bivariate gamma distribution encapsulates the standard gamma distribution in the marginals; but has an additional parameter, called the power correlation parameter  $\rho$ , ( $0 \leq \rho \leq 1$ ), denoting the correlation coefficient of two gamma distributed variates

$$\rho = \frac{\text{Cov}(A_1^2, A_2^2)}{\sqrt{\text{Var}(A_1^2)\text{Var}(A_2^2)}} = \frac{\text{Cov}(p_1, p_2)}{\sqrt{\text{Var}(p_1)\text{Var}(p_2)}}$$

In the equation above,  $A_1, A_2$  denote the amplitude of the signal at time  $T_1$  and  $T_2$ , respectively, and  $p_k = A_k^2$  for  $k = \{1, 2\}$  denotes the power of the signal. The average power is defined as  $\Omega_k = E\{A_k^2\} = E\{p_k\}$ , where  $E\{\cdot\}$  is the expectation operator. It should be remembered that our goal is to study the sequential lobing accuracy when the target amplitudes at times  $T_1$  and  $T_2$  are not fully correlated ( $\rho \neq 1$ ), that is, to quantify the performance loss when the main assumption is violated.

With the presented target model, the return power is modelled as the superposition of  $m$  power components. As can be noted from Fig. 2, when  $m=1$  the general model reduces to Rayleigh model and when  $m=2$ , we have Swerling 3/4 model. The models for higher values of  $m$  can be considered as the generalised Swerling models as suggested in [7].

According to the presented target model, the voltage value of each component contributing to the total received power is complex-valued and circularly symmetric Gaussian distributed with zero mean, unit variance. The target power at times  $t = \{T_1, T_2\}$  can be written as follows

$$p_1 = \sum_{k=1}^m ||x_{1,k}||^2 = \sum_{k=1}^m \left\{ (x_{1,k}^{\text{re}})^2 + (x_{1,k}^{\text{im}})^2 \right\}$$

$$p_2 = \sum_{k=1}^m ||x_{2,k}||^2 = \sum_{k=1}^m \left\{ (x_{2,k}^{\text{re}})^2 + (x_{2,k}^{\text{im}})^2 \right\} \quad (1)$$

In the equation above, the random variables  $x_{1,k} = x_{1,k}^{\text{re}} + jx_{1,k}^{\text{im}}$  and  $x_{2,k} = x_{2,k}^{\text{re}} + jx_{2,k}^{\text{im}}$  denote the complex amplitude of the  $k$ th component contributing to the total received power at time instants  $T_1$  and  $T_2$ , respectively. With the present model, it is assumed that different components, that is, components having different  $k$  indices in (1), are independent from each other; but the return from each component at times  $T_1$  and  $T_2$  are correlated, that is the random variables  $x_{1,k}$  and  $x_{2,k}$ , having identical  $k$  indices, are assumed to be correlated. The sequential lobing technique assumes full correlation between  $x_{1,k}$  and  $x_{2,k}$  leading to the conclusion that  $x_{1,k} = x_{2,k}$ . Our goal is to relax this assumption and examine the performance loss incurred.

For the application of sequential lobing, we may visualise a manoeuvring target which is illuminated twice in a rapid succession. In many systems, the time separation between transmissions is typically a few milliseconds or less. Under these conditions, unless the target is exceptionally agile, the change in the aspect angles of the target reflecting surfaces in between two illuminations is expected to be small. If we assume that the correlation of return powers at two time instants are related to the variations in the illuminated surfaces, there should be a significant correlation between received signals. We may argue that such an explanation is only valid for slowly manoeuvring targets and the performance of sequential lobing is questionable if the manoeuvre is sufficiently rapid.

The correlation between received signal powers  $p_1$  and  $p_2$ , given in (1), can be expressed in terms of the correlation between the individual voltage values  $x_{1,k}$  and  $x_{2,k}$ . If we denote the covariance matrix of  $x_{1,k}$  and  $x_{2,k}$  with  $C_x$ , then the covariance matrix of return powers  $p_1$  and  $p_2$ , denoted with  $C_p$ , can be expressed in a surprisingly compact form [9, eq. (28)] [The eq. (28) in [9] contains an additional factor of 2 which is not required in this paper because of the definition of complex-valued random variables.]

$$C_x = \frac{1}{\sqrt{m}} C_p^{\odot(1/2)} \quad (2)$$

Here,  $A^{\odot(p)}$  denotes the matrix whose elements are the  $p$ th power of the corresponding element of  $A$ , that is,  $(A^{\odot(p)})_{i,j} = (A_{i,j})^p$ . We would like to note that the power correlation parameter  $\rho$  can be experimentally estimated by recording the return power of a manoeuvring target. Once the power correlation is estimated, one can make use of (2) to generate synthetic data for realistic computer simulations.

Finally, we present the joint density of bivariate gamma variables [8, eq. (5)]

$$f_{p_1, p_2}(p_1, p_2) = \frac{m^{m+1}}{\Gamma(m)\Omega_1\Omega_2(1-\rho)} \left( \frac{p_1 p_2}{\rho\Omega_1\Omega_2} \right)^{(m-1)/2}$$

$$\times \exp \left\{ -\frac{m}{1-\rho} \left( \frac{p_1}{\Omega_1} + \frac{p_2}{\Omega_2} \right) \right\} \quad (3)$$

$$\times I_{m-1} \left( \frac{2m}{1-\rho} \sqrt{\rho \frac{p_1 p_2}{\Omega_1 \Omega_2}} \right) u(p_1)u(p_2)$$

Here,  $\Gamma(\cdot)$  is the gamma function,  $I_\alpha(x) = \sum_{k=0}^{\infty} (x/2)^{\alpha+2k} / (\Gamma(\alpha+k+1)k!)$  is the modified Bessel function of order  $\alpha$  and  $u(\cdot)$  is the unit step function. It can be verified that as  $\rho \rightarrow 0$ , the joint density for the random variables  $p_1$  and  $p_2$  approach the product of univariate gamma variables with the following density [8, eq. (3)]

$$f_p(p) = \frac{m^m}{\Omega^m \Gamma(m)} p^{m-1} \exp\left(-\frac{m}{\Omega} p\right) u(p) \quad (4)$$

As a cautionary remark, we would like to note that the bivariate gamma density presented here is known as Jensen’s bivariate gamma distribution in statistics literature [12, p. 438]. There are several other definitions for the bivariate gamma distribution extending the standard gamma density of one random variable to two random variables [12]. Jensen’s density is the natural extension for the radar target modelling encompassing classical Swerling models.

### 3 Sequential lobing technique

The received signal for sequentially switched beam positions can be written as follows

$$\begin{aligned} r_1 &= a_1 P_1(\Theta) + w_1 \\ r_2 &= a_2 P_2(\Theta) + w_2 \end{aligned} \quad (5)$$

Here,  $a_1$  and  $a_2$  represent the complex-valued target amplitude at time instants  $T_1$  and  $T_2$ . The target amplitudes, and therefore the target power values at  $T_1$  and  $T_2$ , are assumed to be correlated. The real-valued functions  $P_1(\Theta)$  and  $P_2(\Theta)$  denote the antenna voltage patterns for two looks. The random variables  $w_1$  and  $w_2$  represent the receiver noise, which are assumed to be independent and Gaussian distributed with zero mean and  $\sigma_w^2$  variance. The SNR of  $k$ th observation is defined as  $\text{SNR}_k = E\{a_k^2\}/\sigma_w^2 = \Omega_k/\sigma_w^2$ . For target modelling, the average power at times  $T_1$  and  $T_2$  is assumed to be the same, that is  $\Omega = \Omega_1 = \Omega_2$ , where  $\Omega$  refers to the average return power of the target and therefore  $\text{SNR} = \text{SNR}_1 = \text{SNR}_2$ . The goal of direction finding is to produce an estimate for the target angular position, that is,  $\hat{\Theta}$ , given the complex-valued measurements  $r_1$  and  $r_2$ .

Sequential lobing technique uses the magnitude of  $r_1$  and  $r_2$  for the estimation of angular position

$$\frac{P_1(\hat{\Theta})}{P_2(\hat{\Theta})} = \frac{|r_1|}{|r_2|} \Rightarrow \hat{\Theta} = f_v^{-1}\left(\frac{|r_1|}{|r_2|}\right) \quad (6)$$

$f_v(\hat{\Theta})$

In the absence of noise, the sequential lobing method produces the true solution, but this technique does not have any optimality properties in the presence of noise; yet it is frequently used in practice. Its practical success can be explained by its close relation with the maximum likelihood (ML) method for non-random (deterministic) targets. The non-random target amplitude does not change in time and therefore can be considered as fully correlated target amplitude ( $\rho=1$ ). The ML estimate for  $\Theta$  given for non-fluctuating and non-random target amplitudes can be written as [13, eq. (5–70)]

$$\frac{P_1(\hat{\Theta}_{\text{ML}})}{P_2(\hat{\Theta}_{\text{ML}})} = \frac{2\text{Re}\{r_1/r_2\}}{\underbrace{1 - |r_1/r_2|^2 + 1 + (r_1/r_2)^2}_{c_r}} \Rightarrow \hat{\Theta}_{\text{ML}} = f_v^{-1}(c_r) \quad (7)$$

$f_v(\hat{\Theta}_{\text{ML}})$

For sufficiently high SNR, that is when the noise variance  $\sigma_w^2$  is sufficiently small in comparison with the average return power from the target, the ML rule approaches  $f_v(\hat{\Theta}) = \text{Re}\{r_1/r_2\} = |r_1|/|r_2| \cos((r_1) - (r_2))$ . Considering high SNR conditions, this relation can be further approximated as  $f_v(\hat{\Theta}) = |r_1|/|r_2|$ , which is the rule for sequential lobing given in (6). Therefore, under the assumption of high SNR, the sequential lobing method approaches ML method for non-fluctuating targets. Further details about the high SNR behaviour of the sequential lobing, ML method and the associated Cramer–Rao lower bound are given in Section 5.

In the present paper, we refer to the ML estimator given in (7) as the monopulse estimator. This monopulse estimator uses both the magnitude and phase information of the received data, and therefore its performance is expected to be better than the sequential lobing method in general. The estimator given in (7) can also be implemented by first forming sum and difference of two receptions ( $r_1$  and  $r_2$ ), which is in some sense equivalent to the formation of sum–difference antenna patterns. Since the formation of sum–difference patterns is an invertible operation, the ML estimate with the sum–difference patterns is identical to the estimate given in (7).

We would like to note that it is not possible to use the ML estimator given in (7) with the sequentially switched beams; since for moving targets, the range change of the target during the beam-switching time causes a phase change which cannot be reliably estimated even for the non-fluctuating targets. This necessitates the use of only the magnitude of the receptions  $r_1$  and  $r_2$  in the target angular position estimation via the sequential lobing method.

### 4 Performance of sequential lobing technique

The sequential lobing estimate  $\hat{\Theta} = f_v^{-1}(|r_1|/|r_2|)$ , given in (6), can equivalently be written in terms of ratio of power patterns  $f_p(\cdot) = [f_v(\cdot)]^2$

$$\hat{\Theta} = f_p^{-1}\left(\frac{|r_1|^2}{|r_2|^2}\right) \quad (8)$$

Here,  $f_p(\Theta) = [f_v(\Theta)]^2 = P_1^2(\Theta)/P_2^2(\Theta)$  is the ratio of antenna power patterns. It should be noted that the estimates produced by the voltage or power patterns are identical. Our preference of power patterns is due to the emergence of simpler analytical expressions for the power variables.

We define the random variable  $p_r$ , which is the power ratio of return signals, as follows

$$p_r = \frac{p_1}{p_2} = \frac{|a_1|^2}{|a_2|^2} \quad (9)$$

In the absence of noise, the received signal model given in (5) simplifies to  $r_1 = a_1 P_1(\Theta)$  and  $r_2 = a_2 P_2(\Theta)$  and the ratio of powers at times  $T_1$  and  $T_2$  can be written as

$$\frac{|r_1|^2}{|r_2|^2} = p_r \frac{P_1^2(\Theta_{\text{true}})}{P_2^2(\Theta_{\text{true}})} = p_r f_p(\Theta_{\text{true}}) \quad (10)$$

Here,  $\Theta_{\text{true}}$  is the true value for the target angular position. For the case of non-fluctuating targets, we have  $p_r=1$  and  $\hat{\Theta} = f_p^{-1}(|r_1|^2/|r_2|^2) = \Theta_{\text{true}}$ . For fluctuating targets, the power ratio  $|r_1|^2/|r_2|^2$  and therefore  $\hat{\Theta}$  are random variables. The mean, variance and the distribution of  $\hat{\Theta}$  determines the performance of direction finding system.

#### 4.1 Distribution of power ratio for fluctuating targets

The ratio of target powers given in (9), where  $p_1$  and  $p_2$  are modelled according to the bivariate-correlated gamma variates given by (3), can be expressed as

$f_{p_r}(p_r) = \int_0^\infty z f_{p_1, p_2}(p_r z, z) dz$  [14, eq. (6–43)]. The analytical expression for  $f_{p_r}(p_r)$  for  $\Omega_1 = \Omega_2$ , can be written as follows [15, eq. (10)] [The condition of  $\Omega_1 = \Omega_2$  utilised in the derivation of (11) relates to the target having the same average power at the time instants of  $T_1$  and  $T_2$  in the present context. Fast fluctuating targets (or equivalently a large time gap between  $T_1$  and  $T_2$ ) may violate this condition. For such targets, the sequential lobing performance is expected to be further degraded.]

$$f_{p_r}(p_r) = \frac{2^{2m-1}}{\sqrt{\pi}(1-\rho)^{-m}} \frac{\Gamma(m+1/2)}{\Gamma(m)} \times \frac{p_r^{m-1}(p_r+1)}{[(p_r+1)^2 - 4\rho p_r]^{m+0.5}} u(p_r) \quad (11)$$

The mean and variance of  $p_r$  can be expressed as follows [11, eq. (2.6)]

$$E\{p_r\} = 1 + \frac{\varepsilon_\rho}{m-1}$$

$$\text{Var}\{p_r\} = \varepsilon_\rho \frac{2}{m-1} + \varepsilon_\rho^2 \frac{(5m-4)}{(m-1)^2(m-2)} \quad (12)$$

In the equation above,  $\varepsilon_\rho = 1 - \rho$  denotes the deviation of the power correlation coefficient from the case of full correlation. Hence, the parameter  $\varepsilon_\rho$  denotes the amount of correlation deficiency. It should be noted that for the fully correlated case ( $\varepsilon_\rho = 0$ ), the target power values at times  $T_1$  and  $T_2$  are identical and their ratio (which is 1) is not a random variable, but a deterministic quantity. As can be noted from (12), when  $\varepsilon_\rho$  is not equal to 0, the mean value of the power ratio is biased from the desired value of 1. Furthermore, the spread around the mean, that is the variance of  $p_r$ , can be infinite if the target is Rayleigh ( $m = 1$ ) or Swerling-4 ( $m = 2$ ) type. This mathematical fact can be easily verified by noting that for large enough  $p_r$  values, the density given in (11) behaves as  $1/p_r^m$ . Hence, the first  $m - 1$  moments are finite and the rest is unbounded. (The probability distributions with unbounded moments are considered as pathological distributions. The Cauchy distribution, whose moments, including the mean, are unbounded, is the most well-known example of the pathological distributions [14].)

The general moment expression for the random variable  $p_r$ ,  $E\{p_r^s\}$ , which is valid not only for the integer values for  $s$  but also for any non-negative real number, can be written as follows [16]

$$\Phi(s) = E\{p_r^s\} = \frac{\Gamma(m+s)(1-\rho)^s}{\Gamma(m)\Gamma(m)} \times \int_0^\infty z^{m-1-s} e_1^{-z} F_1(-s, m; -\frac{\rho}{1-\rho}z) dz, \quad s \geq 0 \quad (13)$$

In the expression above,  ${}_1F_1(a_1, b_1, z)$  is the hypergeometric function [17, 9.100]. It can be verified that for integer values of  $s$  the expression is identical to the one given in [11, eq. (2.6)]. The general moment expression can be

further simplified for  $s < m$  as follows [16]

$$\Phi(s) = E\{p_r^s\} = \frac{\Gamma(m+s)\Gamma(m-s)}{\Gamma(m)\Gamma(m)} {}_2F_1(-s, s; m; \rho), \quad s < m \quad (14)$$

The general moment function valid for real-valued moments is utilised in the next section to calculate the moments of the random variable  $\ln(p_r)$ .

#### 4.2 Performance for Gaussian beam patterns

To quantify the effect of target fluctuation on the sequential lobing (the effect of random variable  $p_r$  on  $\hat{\Theta}$ ), we use commonly selected Gaussian beam patterns. It should be noted that the Gaussian patterns are frequently used in practice and many other practical patterns can be closely approximated with the Gaussian patterns. Previously, we have assumed an arbitrary pattern and expressed the estimate as  $\hat{\Theta} = f_p^{-1}(|r_1/r_2|^2)$ . With the adoption of Gaussian patterns, the function  $f_p(\cdot)$  is written as follows

$$f_p(\Theta) = [f_v(\Theta)]^2 = \left[ \frac{P_1(\Theta)}{P_2(\Theta)} \right]^2 = \left[ \frac{\exp(-a(\Theta/\Theta_{BW})^2)}{\exp(-a([\Theta - \beta\Theta_{BW}]/\Theta_{BW})^2)} \right]^2 \quad (15)$$

The functions  $f_p(\Theta)$  and  $f_v(\Theta)$  are the ratio of power and voltage patterns, respectively. The pattern at the second look has a squint angle of  $\beta\Theta_{BW}$  where  $\Theta_{BW}$  is the half power beamwidth and  $a = 2\ln 2$ .

The estimate via sequential lobing,  $\hat{\Theta} = f_p^{-1}(|r_1/r_2|^2)$ , can be explicitly expressed as follows

$$\hat{\Theta} = \Theta_{BW} \left( \frac{\beta}{2} - \frac{\ln(|r_1|^2/|r_2|^2)}{4a\beta} \right) = c_{BW,\beta} + d_{BW,\beta} \ln \left( \frac{|r_1|^2}{|r_2|^2} \right) \quad (16)$$

Here,  $c_{BW,\beta}$  and  $d_{BW,\beta}$  are constants of the estimator determined by the system beamwidth and the squint angle. Substituting  $|r_1|^2/|r_2|^2 = p_r f_p(\Theta_{true})$  from (10) into (16), the angle estimate can be written in terms of  $\Theta_{true}$

$$\hat{\Theta} = \Theta_{true} + d_{BW,\beta} \underbrace{\ln(p_r)}_{\varepsilon_\theta} = \Theta_{true} + d_{BW,\beta} \varepsilon_\theta \quad (17)$$

Here,  $\varepsilon_\theta = \ln(p_r)$  and the random variable  $p_r$  is the ratio of target power at times  $T_1$  and  $T_2$  whose density is defined in (11). It is interesting to note that the random variable  $p_r$ , appearing as a multiplicative noise term in (10), acts as an additive noise term on the final angle estimate in (17).

To study the effect of amplitude fluctuation on  $\hat{\Theta}$ , we need to examine the statistics of  $\varepsilon_\theta = \ln(p_r)$ . The density of  $\varepsilon_\theta$  can be expressed in terms of the density of  $p_r$  as  $f_{\varepsilon_\theta}(\varepsilon_\theta) = f_{p_r}(e^{\varepsilon_\theta})e^{\varepsilon_\theta}$ . For the characterisation of the sequential lobing accuracy, we need first two moments of  $\varepsilon_\theta$ . Unfortunately, the moments of  $\varepsilon_\theta$  are difficult to calculate directly and we utilise the moment function of  $p_r$ , denoted as  $\Phi(s)$  in (14), to calculate the moments of  $\varepsilon_\theta = \ln(p_r)$ .

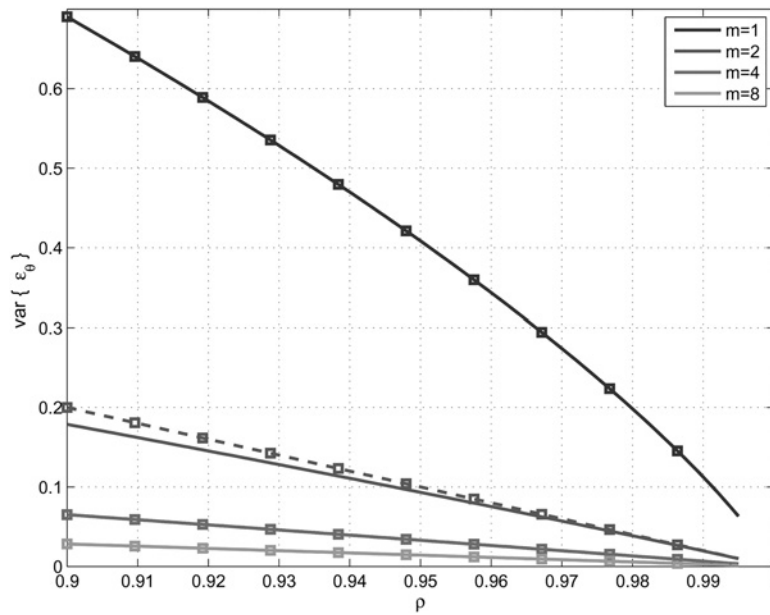


**Fig. 3** Comparison of error variance formula (19) (solid line) and its high correlation approximation (20) (dashed line with square marker)

The  $k$ th derivative of  $\Phi(s) = E\{p_r^s\}$  can be written as follows

$$\frac{d^k}{ds^k} \Phi(s) = \Phi^{(k)}(s) = E\left\{p_r^s [\ln(p_r)]^k\right\} \quad (18)$$

By evaluating the expression above at  $s = 0$ , we can get the  $k$ th integral moment of  $\ln(p_r)$ . It should be noted that to evaluate the derivatives of  $\Phi(s) = E\{p_r^s\}$  at  $s = 0$ , the function  $\Phi(s)$  should be expressed for a continuum of values around 0.

The first moment of  $\varepsilon_\theta$ , which is the mean, is equal to  $\Phi^{(1)}(0)$ . It can be noted from (13) that  $\Phi(s)$  is an even function. Therefore all odd-order moments are equal to zero. Since the first moment is zero, we can conclude that the sequential lobe estimates are unbiased. For the variance of  $\varepsilon_\theta$ , the second derivative of  $\Phi(s)$  should be calculated. Care must be exercised to evaluate the second derivative, since the differentiation is with respect to the parameters of the hypergeometric function in (14), but not with respect to its argument. After some algebra, we obtain the expression for the variance as follows

$$\begin{aligned} \text{Var}(\varepsilon_\theta) &= \Phi^{(2)}(0) = 2\Psi^{(1)}(m) + \left. \frac{d^2}{ds^2} {}_2F_1(-s, s; m; \rho) \right|_{s=0} \\ &= 2\left[\Psi^{(1)}(m) - \frac{\rho}{m} {}_3F_2(1, 1, 1; 2, m + 1; \rho)\right] \end{aligned} \quad (19)$$

In the equation above  $\Phi^{(1)}(\cdot)$  is the first derivative of the

digamma function, also known as the psi function. The exact expressions given above are difficult to interpret because of the appearance of special functions. An approximation for the variance formulas around  $\rho \simeq 1$  can be given by expressing the hypergeometric function in (19) as a power series at  $\rho = 1$  (see (20))

The dilogarithm function, appearing in the first line of (20), is a transcendental function with the definition  $\text{dilog}(x) = \int_1^x (\ln t/1 - t)dt$ . The parameter  $\varepsilon_\rho$  has the definition of  $\varepsilon_\rho = 1 - \rho$  and shows the amount of correlation deficiency. The phrase h.o.t. denotes higher order terms. It should be noted that the case of  $m = 1$  in (20) is exact, that is, there are no higher order terms for this case.

Fig. 3 is generated to check the accuracy of suggested approximation for the high correlation region. The high correlation approximations are particularly valuable for the analysis of the sequential lobing technique, since the power correlation is expected to be high for this application. Furthermore, the evaluation of hypergeometric function appearing in the exact relation (19) converges slowly for  $\rho$  values close to 1 and the approximate formulas can also be preferred to speed up some numerical calculations.

### 5 Regimes of operation and numerical results

Three sets of numerical results are provided to quantify the effect of amplitude fluctuation on the accuracy of sequential lobing. The first set shows the performance in the absence

$$\text{Var}(\varepsilon_\theta) = \begin{cases} \frac{\pi^2}{3} - 2\text{dilog}(\varepsilon_\rho), & m = 1 \\ \frac{2}{m-1} \varepsilon_\rho + \text{h.o.t.}, & m = 2 \\ \frac{2}{m-1} \varepsilon_\rho - \frac{1}{(m-1)(m-2)} \varepsilon_\rho^2 + \text{h.o.t.}, & m = 3 \\ \frac{2}{m-1} \varepsilon_\rho - \frac{1}{(m-1)(m-2)} \varepsilon_\rho^2 + \frac{4}{3(m-1)(m-2)(m-3)} \varepsilon_\rho^3 + \text{h.o.t.}, & m \geq 4 \end{cases} \quad (20)$$

of receiver noise. This set solely shows the effect of target fluctuation on the sequential lobe estimate; in other words, this set examines the deviation from true value because of target amplitude fluctuations. The second set contains receiver noise in addition to the amplitude fluctuation and examines the joint effect of noise and amplitude fluctuation at different SNR levels. The third set illustrates different regimes of operation. In the first regime, the performance is limited by the target fluctuation, whereas in the second one, the performance is limited by the noise. An analytical expression for the SNR boundary between two regimes is also given. Finally, a discussion is given to evaluate the value of sequential lobing method for a target with known fading parameter.

For numerical experiments, a Gaussian beam switched between two positions having an offset angle of  $0.5 \times BW$  ( $BW$  is the beamwidth) and a target with the angular position of  $0.25 \times BW$  is assumed. The estimates for the sequential lobing technique are generated using (16) where  $|r_k|^2$  is the received signal power at the  $k$ th position of the antenna. (For the described system, the parameters of the estimator (16) are  $c_{BW,\beta} = 0.25$  and  $d_{BW,\beta} = -0.36$ ).

5.1 Set 1: Sequential lobing performance in the absence of receiver noise

Fig. 4 shows the performance of the sequential lobing technique in the absence of noise. This figure and subsequent figures show the root-mean-square (RMS) value of the angle estimate error against the power correlation parameter. The target is assumed to have a fading parameter  $m = \{1, 2, 4, 8\}$ . The solid lines in Fig. 4 show the result of Monte Carlo simulations. The dashed lines with square markers are the square root of the analytical results given in (20). It should be noted from this figure that the solid and dashed lines completely overlap except for the case of  $m = 2$ . The deviation for this

case is due to the approximate nature of (20). When the exact variance formulas given in (19) are used instead of the approximate ones, the solid and dashed lines completely overlap for all cases. Here we use the approximate formulas, with elementary mathematical functions, instead of the exact relations with the special functions, to analytically examine different regimes of operation.

In Fig. 4, the performance of the random pick system producing the angle estimate by randomly picking an angle within the beamwidth is also given. The random pick is assumed to have a density which is uniformly distributed density in  $[-BW/2, BW/2]$  and therefore the RMS error for random pick is  $1/\sqrt{12} \times BW \simeq 0.288 \times BW$ . The random pick system acts as a worst-case benchmark for other estimators. It must be noted that the estimates of the sequential lobing algorithm defined by (16) are not confined within the antenna beamwidth.

One can conclude from Fig. 4 that a Rayleigh fluctuating target ( $m = 1$ ) having the power correlation of  $\rho = 0.91$  has an RMS error identical to the random pick system. Hence, targets having a power correlation smaller or equal to 0.91 are not estimated better than the random pick system with the application of the sequential lobing. It should be remembered that there is no receiver noise in the present set of results. Hence, the observed performance degradation is 'solely' because of target fluctuation which is an effect not accounted in the sequential lobing system model. The present results for the Rayleigh model show that the sequential lobing is not robust to this unaccounted effect. The degradation can be more significant when noise is present in addition to the amplitude fluctuation.

It can be observed from Fig. 4 that targets having larger fading parameter ( $m$ ) are more robust to the effects of amplitude fluctuation. As noted before, the parameter  $m$  of the target models shown in Fig. 2, essentially represents the levels of amplitude spread because of target fluctuation. Models with small  $m$  values are the classical Swerling models and as  $m$  increases, the target is considered to

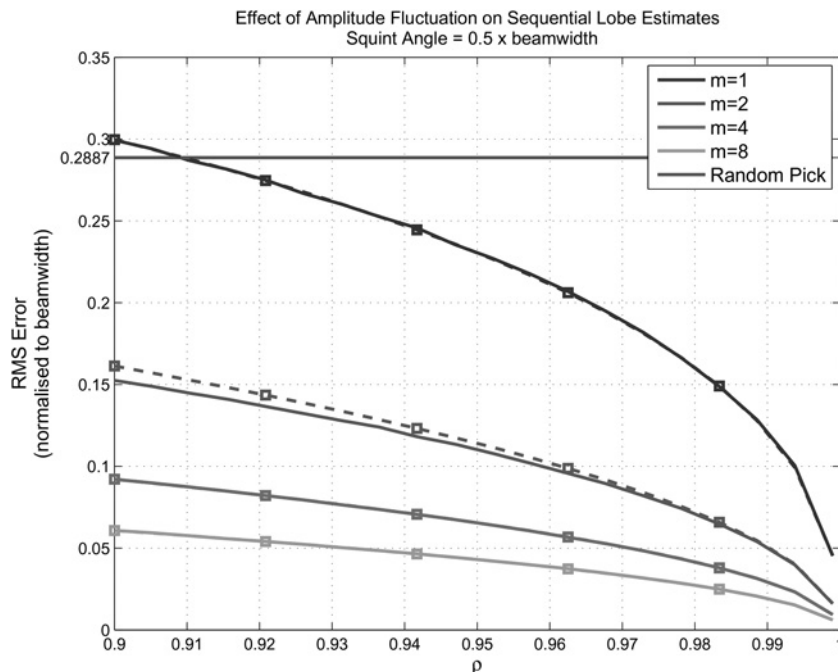
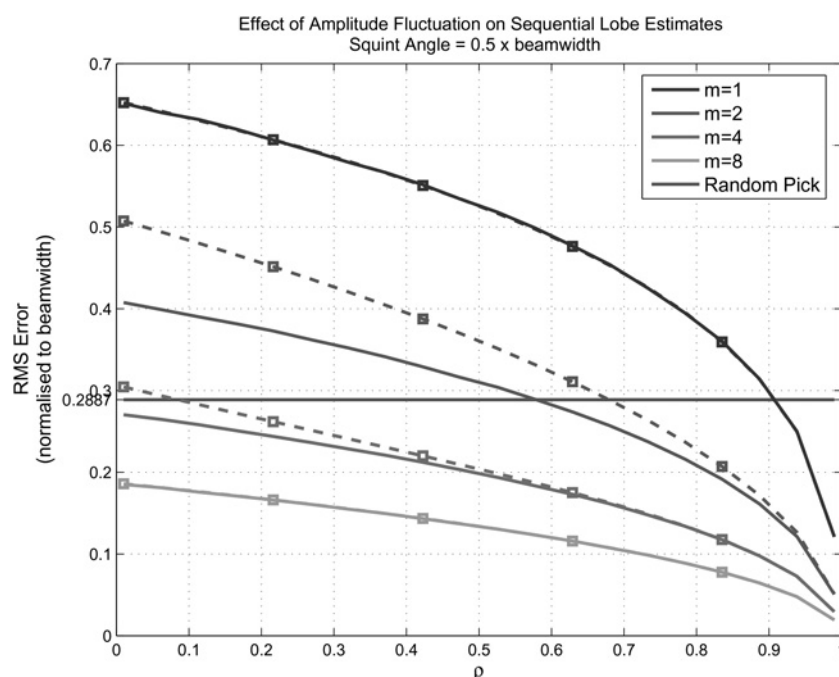


Fig. 4 Performance degradation of sequential lobing technique because of target fluctuation

Solid lines are the results of Monte Carlo simulations, the dashed lines with square markers are the analytical results given by (20)



**Fig. 5** Performance degradation of sequential lobing technique because of target fluctuation for a wide range of correlation values  
Solid lines are the results of Monte Carlo simulations, the dashed lines with square markers are the analytical results given by (20)

approach the non-fluctuating state, making the sequential lobe estimates more accurate.

Fig. 5 presents the results of a similar study for a wide range of correlation values. As noted before, the sequential lobing method operates with the implicit assumption of  $\rho = 1$  (fully correlated echos); in this work, we examine the performance degradation when this condition is violated. In many scenarios, the correlation values smaller than 0.9 can be considered as too low for the application of the sequential method; yet, we present the results given in Fig. 5 to further emphasise the importance of the power correlation assumption.

The dashed lines with the square markers in Fig. 5 are the results of analytical results given by (20); the solid lines are the results of Monte Carlo simulations. For the case of  $m = 1$ , the expression given in (20) is exact and the Monte Carlo runs are in perfect accord with the analytical results. For the other cases, the analytical results are approximations valid for  $\rho \simeq 1$ , hence there is some deviation between dashed and solid lines for small correlation values. Note that the exact error variance relation valid for all cases is present in (19). We prefer the approximate relation given by (20) because of its simpler analytical structure. It should be noted that the deviation is quite limited at high correlation, which is the case of importance for the application of sequential lobing. Furthermore, it can be noted that as target amplitude becomes more stable, that is as  $m \rightarrow \infty$ , the impact of the amplitude fluctuation on the RMS error is reduced.

## 5.2 Set 2: Sequential lobing performance in the presence of receiver noise

The second set of results starts with Fig. 6. This figure shows the performance of the system at SNR = 30 dB. SNR value refers to the detection SNR which is the SNR value after the completion of beamforming, slow- and fast-time processing. In this figure, the performance of the monopulse system is also given. The monopulse system is assumed to implement

the ML estimator given in (7). Monopulse system is not affected by the amplitude fluctuation. The analytical expressions for the performance of monopulse system is rather complicated; but can be found for standard Swerling models in [18]. The monopulse results are presented as lower bounds for the sequential lobing results and they are generated through Monte Carlo simulations.

In Fig. 6, the dashed lines with square markers are the analytical results for the *noiseless* case. The solid lines in this figure show the result of Monte Carlo runs having both noise and amplitude fluctuation. Our goal in this figure is to compare the effect of noise on the sequential lobe estimates, that is, to examine the performance difference between dashed and solid lines.

It can be argued from Fig. 6a that the performance of the sequential lobing technique is not significantly deviated from noise-free case for SNR = 30 dB. An important point to note is that when noise is present, it is not possible to reduce the error of sequential lobing method to arbitrarily small values as  $\rho \rightarrow 1$ . The RMS error of the sequential lobing estimates are lower bounded by the performance of the monopulse system which has the error of 0.0228 units. As  $\rho \rightarrow 1$ , the RMS error for the sequential lobe estimates goes to this limit.

Fig. 6b shows the high correlation region of Fig. 6a, which is the region of interest for the sequential lobing. One important conclusion from Fig. 6b is that for  $m = 1$  (Rayleigh fluctuating targets), the dominant error source affecting the angle estimation is the target fluctuation. This conclusion can be justified by noting the smallness of deviation between dashed and solid lines and at the same time, the significant deviation of both lines from the monopulse bound for  $m = 1$ . Hence, in comparison with the monopulse system, some performance loss is expected for Rayleigh fluctuating targets even at SNR = 30 dB.

If we focus on the case of  $m = 2$  in Fig. 6b and compare the dashed curve (noiseless operation) with the monopulse bound, we can note that the error cannot be reduced below a certain

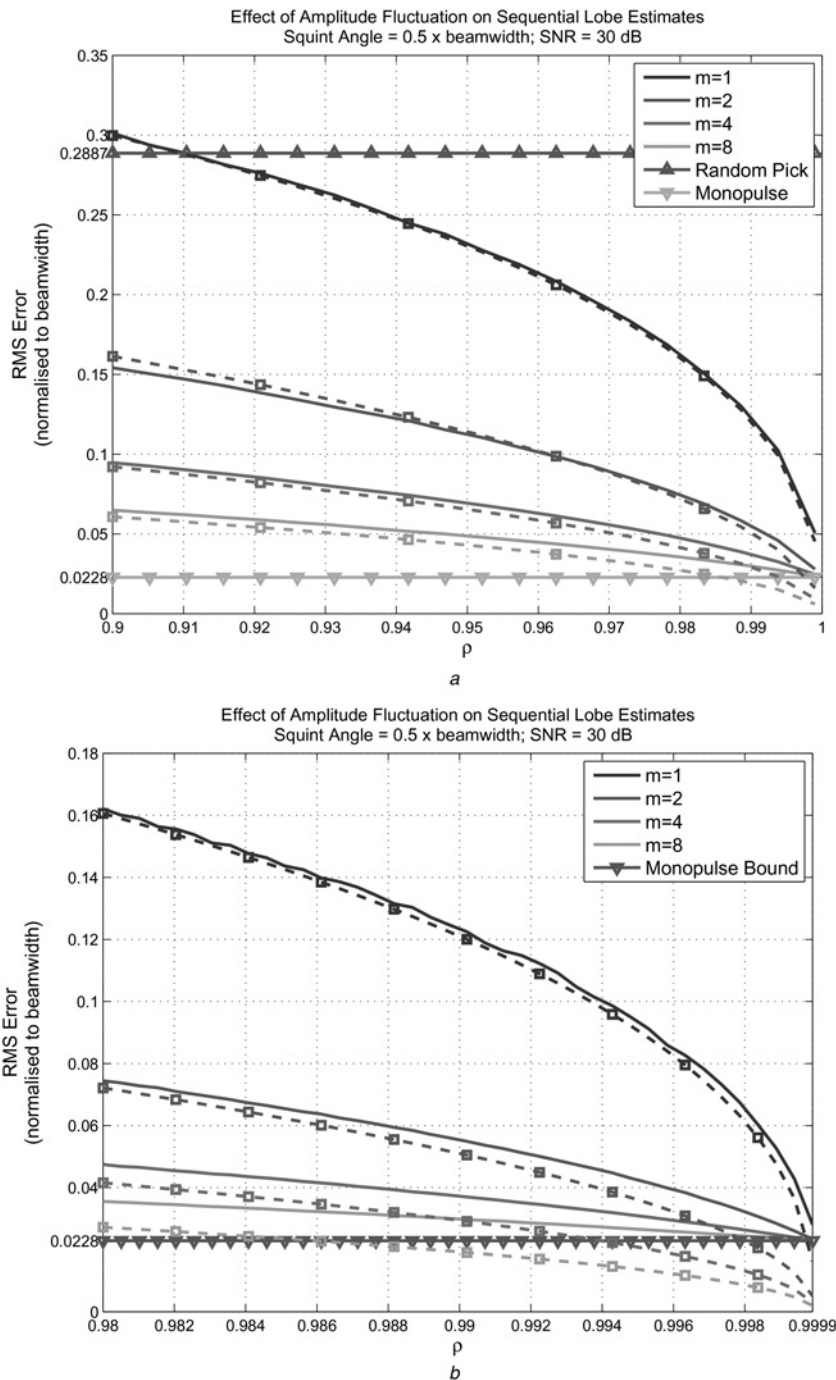


**Fig. 6** Performance of sequential lobing technique because of target fluctuation and receiver noise

Dashed lines show noiseless performance, solid lines show the performance at SNR = 30 dB

a RMS Error vs. Power Correlation  
b High Correlation Region ( $\rho \geq 0.98$ )

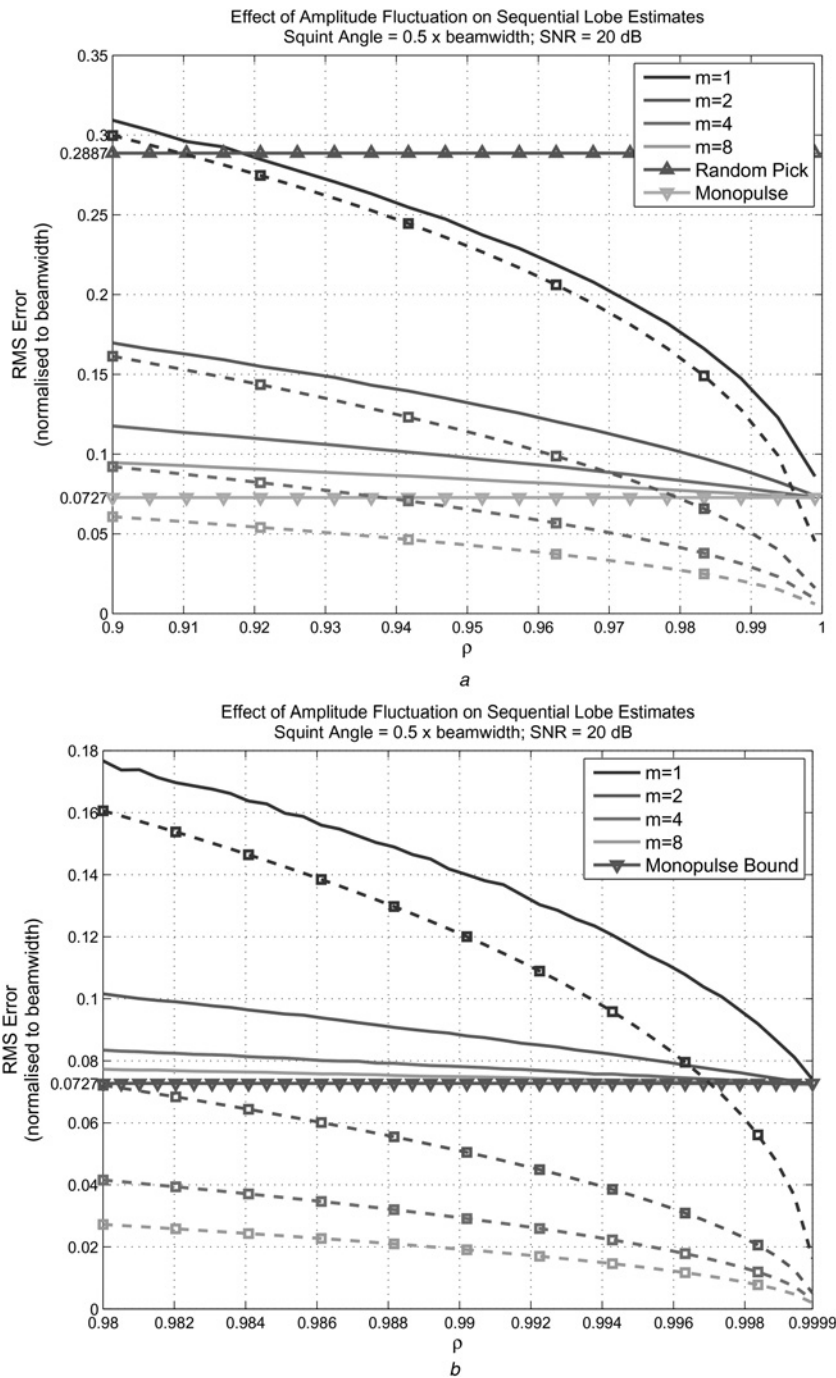
limit when  $\rho$  is  $>0.998$ . Hence, the term dominating the estimation error for  $\rho > 0.998$  is the system noise. On the other hand, for smaller values of  $\rho$ , say  $\rho = 0.99$ , the performance for noisy (solid line) and noiseless (dashed line) cases are very close and it can be said that the performance loss is mainly because of the target fluctuation. This discussion gives us a hint of different regimes of operation.

Fig. 7 repeats the same experiment for SNR = 20 dB. The high correlation region given in Fig. 7b suggests that the system performance is significantly affected by the noise. The dashed curves (noise-free operation) are almost entirely (except for  $m = 1$ ) below the monopulse bound indicating that the actual performance cannot approach the noiseless

case in the high correlation region. As a conclusion for this case, we can say that at SNR of 20 dB and  $\rho > 0.98$ , the system performance is dominated by noise (not by amplitude fluctuation).

### 5.3 Set 3: Regimes of operation

Figs. 6 and 7 show the operation of the sequential lobing system at two different SNR values. From Fig. 6, we note that the performance of sequential lobing for a target with the power correlation of  $\rho = 0.99$  and SNR = 30 dB is essentially determined by the amplitude fluctuation. This result is contrary to the conclusion derived for the same



**Fig. 7** Performance of sequential lobing technique because of target fluctuation and receiver noise

Dashed lines show noiseless performance, solid lines show the performance at SNR = 20 dB

a RMS Error vs. Power Correlation  
b High Correlation Region ( $\rho \geq 0.98$ )

target at SNR of 20 dB. From the presented discussions, it should be clear that there are two different regimes of operation, namely the noise-limited and the target-fluctuation-limited operation specific for the sequential lobing method. In the third set of results, we examine these regimes and determine the boundary between two regimes.

In Fig. 8, we present the RMS error for both sequential lobing and monopulse techniques at different SNR values.

This figure is generated for non-fluctuating targets ( $\rho = 1$ ). The associated Cramer–Rao lower bound is also given. An analytical expression of the error variance for both methods is difficult to express because of the non-linearities appearing in the estimators, but the Cramer–Rao bound (CRB) for this problem can be fairly easily calculated as follows (see (21)).

It can also be observed from Fig. 8 that the performance of

$$CRB(\Theta_{true}) = \frac{1}{2SNR} \left[ \left( \frac{d}{d\Theta_{true}} \{P_1(\Theta_{true})\} \right)^2 + \left( \frac{d}{d\Theta_{true}} \{P_2(\Theta_{true})\} \right)^2 \right], \quad \begin{matrix} \text{(no target fluctuation)} \\ \text{(only system noise)} \end{matrix} \quad (21)$$

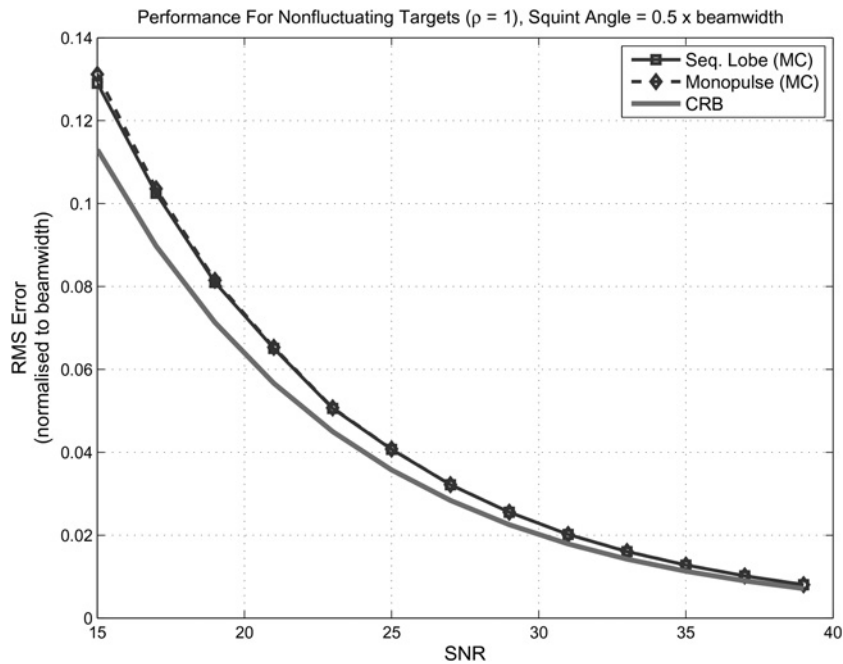


Fig. 8 RMS error of monopulse, sequential lobing techniques and the associated Cramer–Rao lower bound

both methods and CRB is almost identical for SNR > 15 dB. This suggests to use the analytical relation for CRB, given above, as a substitute for the error variance of the estimators.

We note that CRB given in (21) is derived in the absence of target fluctuation and the system noise is the only term affecting the estimation error. Hence, CRB result indicates the performance of noise-limited operation.

For other operational regime, the error variance solely because of target fluctuation is needed. The error variance for this regime can be written, using the first-order approximation in (20) as follows

$$\text{Error variance} = d_{\text{BW},\beta}^2 \frac{2}{m-1} \varepsilon_\rho, \quad \left( \begin{array}{l} \text{only target fluctuation} \\ \text{no system noise} \end{array} \right) \quad (22)$$

The presented approximation is valid for  $m \geq 2$  and  $\rho \simeq 1$ . The factor  $d_{\text{BW},\beta}$  is the scaling factor utilised in (16).

The boundary for the operational regimes can be set by equating the analytical expressions given in (21) and (22) to each other. It can be said that at the boundary point, the effect of target fluctuation is identical to the effect of noise. Equating these two equations, we obtain the following relation (see (23)).

In this relation, the value of  $\varepsilon_\rho$  (the correlation deficiency) is compared with the quantity on the right-hand side of (23). Depending on the pointing direction of the inequality sign, the regime of sequential lobing, noise-limited or target-fluctuation-limited, is determined. It is interesting to note that for  $m = 1$  (Rayleigh fluctuating targets), the sequential lobing suffers from target fluctuation irrespective of SNR value, confirming earlier findings in Set 2. For  $m = 2$  and at SNR values of 30 and 20 dB (as in Figs. 6

and 7), the formula accurately predicts the boundaries as  $\rho$  as 0.9985 and 0.9846, respectively.

## 6 Summary and conclusions

The sequential lobing method operates with the implicit assumption of fully correlated echos ( $\rho = 1$ ). In this work, we examine the performance degradation when this assumption is violated. To this aim, a fairly comprehensive statistical target fluctuation model, which can be denoted as the generalised Swerling model, is utilised.

The insightful picture given by Skolnik [1, Fig. 4.16], which is believed to be based on empirical observations, has initiated the present work. With this picture, Skolnik shows different error sources acting on the angle estimates and compares the impact of these sources on the sequential lobing and monopulse techniques. To the best of our understanding, this figure is presented as a qualitative description of the relations arising from the experience of Skolnik. One of the major goals of this study is to quantify this picture via recently suggested statistical target models.

Our findings closely agree with the conclusions of Skolnik. One important result, which is absent in the Skolnik’s descriptions, is for Rayleigh fluctuating targets (when fading parameter  $m$  is equal to 1), the amplitude fluctuation is the dominant component contributing to the error of the sequential lobing technique. Hence, the sequential lobing cannot yield a performance similar to monopulse techniques at any SNR or power correlation coefficient for such targets. For targets having less amplitude spread because of the target fluctuation, that is, when  $m \geq 2$ , the situation is more promising. For such targets, there are two regimes of operation, namely the noise-limited regime and the target-fluctuation-limited regime as described in the present paper.

$$\varepsilon_\rho \stackrel{\text{Noise}}{\underset{\text{Fluctuation}}{\leq}} \frac{m-1}{4\text{SNR } d_{\text{BW},\beta}^2} \left[ \left( \frac{d}{d\Theta_{\text{true}}} \{P_1(\Theta_{\text{true}})\} \right)^2 + \left( \frac{d}{d\Theta_{\text{true}}} \{P_2(\Theta_{\text{true}})\} \right)^2 \right] \quad (23)$$

As an illustration of the quantitative results presented herein, we can say that a target with an SNR of 20 dB and having an amplitude fluctuation model with fading parameter  $m=2$  has a direction finding error dominated by the target amplitude fluctuation when its received power correlation between two looks of sequential lobing is less than 0.9846. Similar results can be produced for different target fluctuation models. Furthermore, the boundaries between noise-limited and amplitude-fluctuation-limited regimes can be analytically expressed either in terms of power correlation for a given SNR or in terms of SNR for a given power correlation.

The present work can be useful to assess the engineering utility of sequential lobing. It is clear that some amount of target fluctuation is unavoidable for the sequential lobing. If the performance of the sequential lobing system is comparable with the performance of monopulse systems for typical SNR and power correlation values, the system designer may prefer the sequential lobing implementation over the monopulse implementation because of its modest hardware requirements.

## 7 References

- Skolnik, M.I.: 'Introduction to radar systems' (McGraw-Hill, New York, 2001, 3rd edn.)
- Lo, K.W.: 'Theoretical analysis of the sequential lobing technique', *IEEE Trans. Aerosp. Electron. Syst.*, 1999, **35**, (1), pp. 282–293. ISSN 0018-9251
- Cui, G., Maio, A.D., Pallotta, L., Farina, A.: 'Theoretical analysis of the sequential lobing technique for correlated targets', *IET Radar Sonar Navig.*, 2013, **7**, (4), pp. 443–450
- Bullock, L.G.: 'An analysis of wide-band microwave monopulse direction-finding techniques', *IEEE Trans. Aerosp. Electron. Syst.*, 1971, **7**, (1), pp. 188–203
- Leonov, A.I., Fomichev, K.I.: 'Monopulse radar' (Artech House, New York, 1986)
- Nickel, U.: 'Overview of generalized monopulse estimation', *IEEE Aerosp. Electron. Syst. Mag.*, 2006, **21**, (6), pp. 27–56
- Cui, G., DeMaio, A., Piezzo, M.: 'Performance prediction of the incoherent radar detector for correlated generalized Swerling-chi fluctuating targets', *IEEE Trans. Aerosp. Electron. Syst.*, 2013, **49**, (1), pp. 356–368
- Piboongunon, T., Aalo, V.A., Iskander, C.D., Efthymoglou, G.P.: 'Bivariate generalised gamma distribution with arbitrary fading parameters', *Electron. Lett.*, 2005, **41**, (12), pp. 709–710. ISSN 0013-5194
- Zhang, Q.T.: 'A decomposition technique for efficient generation of correlated Nakagami fading channels', *IEEE J. Sel. Areas Commun.*, 2000, **18**, (11), pp. 2385–2392. ISSN 0733-8716
- Yacoub, M.D., Bautista, J.E.V., Guerra de Rezende Guedes, L.: 'On higher order statistics of the Nakagami-m distribution', *IEEE Trans. Veh. Technol.*, 1999, **48**, (3), pp. 790–794. ISSN 0018-9545
- Tubbs, J.D.: 'Moments for a ratio of correlated gamma variates', *Commun. Stat. – Theory Methods*, 1986, **15**, (1), pp. 251–259
- Kotz, S., Balakrishnan, N., Johnson, N.L.: 'Continuous multivariate distributions volume 1: models and applications' (John Wiley & Sons, New York, 2000)
- Zoltowski, M.D.: 'Adaptive radar detection and estimation', chapter 5: Beam-space ML bearing estimation for adaptive phased array radar (John Wiley and Sons, 1992), pp. 237–332
- Papoulis, A.: 'Probability, random variables, and stochastic processes' (McGraw-Hill, New York, 1991, 3rd edn.)
- Bithas, P.S., Sagias, N.C., Tsiftsis, T.A., Karagiannidis, G.K.: 'Distributions involving correlated generalized gamma variables'. Proc. Int. Conf. Applied Stochastic Models and Data Analysis, 2007, vol. 12, pp. 1–8
- Candan, C., Orguner, U.: 'The moment function for the ratio of correlated generalized gamma variables', *Elsevier Stat. Probab. Lett.*, 2013, **83**, (10), pp. 2353–2356
- Gradshteyn, I.S., Ryzhik, I.M.: 'Table of integrals, series and products' (Academic Press, USA, 2007, 7th edn.)
- Nickel, U.R.O., Chaumette, E., Larzabal, P.: 'Statistical performance prediction of generalized monopulse estimation', *IEEE Trans. Aerosp. Electron. Syst.*, 2011, **47**, (1), pp. 381–404. ISSN 0018-9251